Report on a problem studied at the UK Mathematics-in-Medicine Study Group Reading 2011
< http://www.maths-in-medicine.org/uk/2011/asthma/ >

Mathematics in Medicine Study Group, Reading 2011

Mathematical modelling of airway smooth muscle cell proliferation and apoptosis in asthma

Authors: M. Baker[1], L. Chapman[2], Dr I. Chernyavsky[1,3], Dr H. Croisier[1,0], L. Gallimore[2], J. Hiorns[1], Dr A. Holmes[7], Dr J. Phillips[4], T. Snowden[5]

Problem Presenters: Dr C. Billington[6], Prof I. Hall[6], Dr A. Holmes[7], Prof S. Johnson[6]

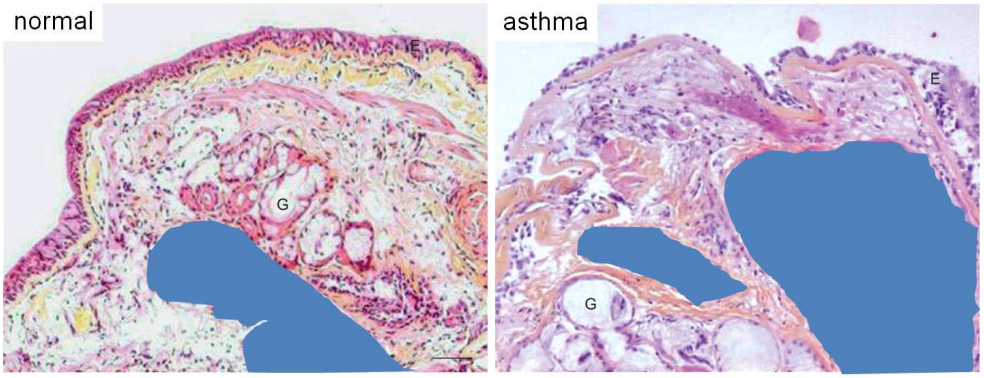

Bara, et al. European Respiratory Journal, 2010
(Airway smooth muscle shown in blue)

[1] School of Mathematical Sciences, University of Nottingham
[2] Mathematical Institute, University of Oxford
[3] DAMTP, University of Cambridge
[4] Department of Mathematics, University College London
[5] Department of Mathematics and Statistics, University of Reading
[6] Department of Therapeutics and Molecular Medicine, University of Nottingham
[7] National Centre for the Replacement, Refinement and Reduction of Animals in Research (NC3Rs)

[0]Report coordinator.

1 Challenge outline

Asthma is a chronic, inflammatory disease of the airways, characterised by airway hyper-responsiveness (increased airway smooth muscle contractility) and remodelling (airway structural changes, including airway smooth muscle proliferation). It affects five million people in the UK alone, and whilst many of these will have only mild disease, there are over 1300 deaths due to asthma each year [2]. Additionally, with many sufferers on long term medication and over 70,000 hospital admissions per year, this disease places a large financial burden on health services [2].

Despite much research interest and many pre-clinical successes, little progress has been made in finding clinically effective treatments to halt the progression of the disease. The failure to translate promising drug candidates from animal models to humans has led to questions about the utility of the *in vivo* studies and demand for more predictive models and tools based on the latest technologies. To facilitate progress, the UK NC3Rs (National Centre for the Replacement, Refinement, and Reduction of animals in Research) has identified and is supporting several research priorities [21] to reduce reliance on animal models, one of which is the greater use of mathematical modelling, which may be able to provide some insight into why pre-clinical successes are not being translated into effective treatment.

In accordance with this, the following challenge was submitted to the 2011 MMSG:

- Demonstrate that the airway smooth muscle (ASM) proliferation rates observed *in vitro* cannot govern proliferation *in vivo* on a constant-growth-rate basis, because airway remodelling *in vivo* occurs on a much slower timescale than ASM cell proliferation *in vitro* ;
- Determine the extent to which proliferation and apoptosis participate in the turnover rates of human ASM cells in normal and diseased tissue; i.e., determine the ratio of proliferation to reduced apoptosis necessary to account for the observed ASM mass increase in asthma;
- Quantify the effect of ASM mass increase on the greater reduction of lung function over lifetime observed in people with asthma.

2 Challenge details

The lungs are responsible for the oxygenation of the blood and for the removal of carbon dioxide. Within the lungs, there is a branching network of airways, which go from the trachea to the alveoli. There are 23 generations of airways, with the first sixteen (conducting airways) being responsible for warming and moistening the air and removing any foreign objects that could infect the lungs. The other seven generations are the transitional and respiratory airways, wherein gas is exchanged [1, 13].

A number of different cell types form the airway wall. Figure 1 shows an image of a section of the lung with some of these cells shown. Epithelial cells line the airways and have hair-like protrusions called cilia. Goblet cells are found interspersed between the epithelial cells with the function of secreting mucus. Inhaled particles are trapped in the mucus and then transported towards the mouth by the beating cilia [12]. Beneath the epithelial cells is the basement membrane, and then there is a region made up of smooth muscle and connective tissue including collagen and elastin. In large airways, support

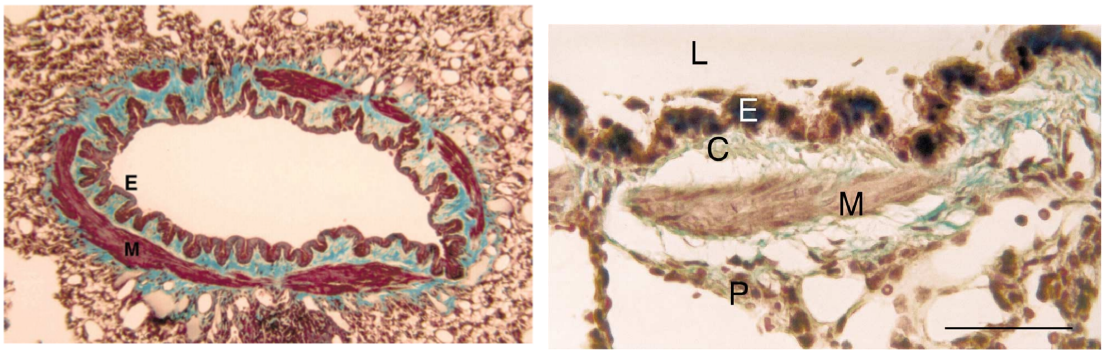

Figure 1. *Left: constricted rabbit airway cross section with mucosal folding. Right: section of a constricted rabbit bronchial ring. L, lumen; E, epithelial-basement membrane layer; C, collagen-rich fibres; M, muscle; P, parenchyma. Reproduced from [24].*

is also provided by cartilage. Smooth muscle cells are spindle-shaped [24] and grouped together to form a bundle of cells.

People with asthma undergo exacerbation events, during which signals are sent to the ASM cells, which induce their contraction, and so cause (reversible) narrowing of the airways. A range of triggers (depending on the patient) can initiate this process, including allergens such as dust mites, inhaled irritants such as cigarette smoke or weather conditions such as cold air. The resulting symptoms include coughing, wheezing and feeling breathless.

Recurrent exacerbation episodes can damage the airways. Indeed, as a part of the healing process, various cytokines and growth factors are released, which induce remodelling of the airway. This includes the following irreversible changes (fig. 2):

- Goblet cell hyperplasia (i.e. proliferation of mucus secreting cells) in both the proximal airways and the smaller airways, where they are normally scarce or absent;
- Thickening of the basement membrane, and deposition of extracellular matrix, including collagen and fibronectin [6];
- Increased ASM mass, through ASM cell hyperplasia and hypertrophy (increase in cell size).

Whereas in healthy individuals, the ASM mass is essentially constant, in fatal asthma, a three-fold increase in ASM mass and cell count has been observed in airways with a diameter greater than 1mm [10, 19]. This increase is also reported by Bai *et al.* [3] (see table in Figure 3). The effect on the thickness and the resulting narrowing is relatively large in the small airways. Although ASM cell hypertrophy has been observed, hyperplasia is believed to play a much larger role in ASM mass increase [14], hence the focus of the challenge on ASM cell proliferation and apoptosis.

Lung function is usually measured by the forced expiratory volume in one second (FEV_1), which is the volume of air a patient can exhale in the first second following a deep breath. In a healthy adult, the FEV_1 gradually decreases with age due to a reduction in the chest wall compliance [30]. In people with asthma, the decrease is more rapid, although it can depend on the severity of asthma. Figure 4 shows the rate of decline of FEV_1 for healthy individuals and individuals with asthma. Figure 5 shows

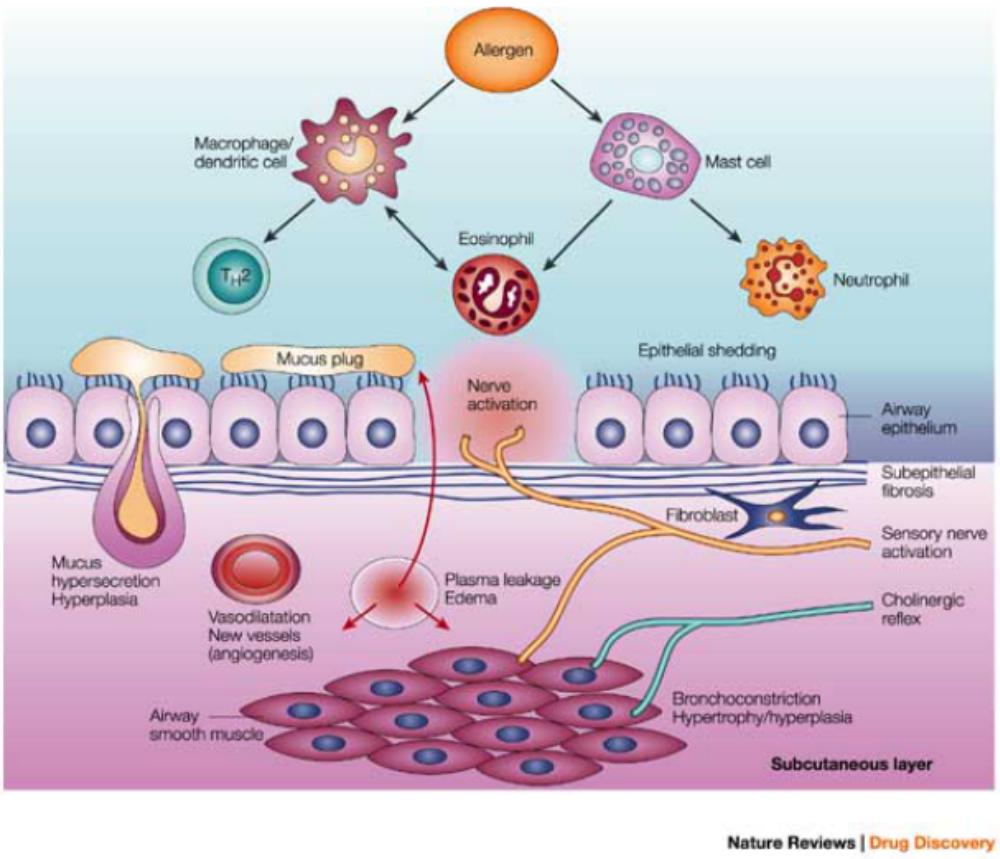

Figure 2. *During an asthma attack, a number of inflammatory cells release inflammatory mediators, which lead to remodelling of the airways. This includes increased numbers of blood vessels and goblet cells and an increase in ASM mass. Reproduced from [4].*

AIRWAY SMOOTH MUSCLE COMPONENTS

Group	n	Mean Pbm (*mm* ± *SE*)	Smooth Muscle Area Fraction (% ± *SE*)	Area Fraction Smooth Muscle per Bundle (% ± *SE*)	Smooth Muscle (mm^2 ± *SE*)
Controls					
Young	5	4.4 ± 0.5	12.3 ± 2.8	92.2 ± 4.0	0.09 ± 0.14
Old	6	4.5 ± 0.5	15.9 ± 2.6	89.6 ± 3.7	0.11 ± 0.13
Asthmatic					
Young	13	4.5 ± 0.5	17.9 ± 1.8*	83.8 ± 2.5†	0.18 ± 0.08*,§
Old	10	5.1 ± 0.6	21.2 ± 2.1*	77.6 ± 3.8†	0.45 ± 0.10*,‡

Definition of abbreviation: Pbm = basement membrane perimeter.
* $p < 0.04$, all individuals with asthma versus all control subjects.
† $p < 0.003$, all individuals with asthma versus all control subjects.
‡ $p = 0.04$ versus age-matched control subjects.
§ $p = 0.07$ versus age-matched control subjects.

Figure 3. *Table showing that the amount of ASM remains almost constant over lifetime in healthy individuals while a 2.5-fold increase is observed in people with asthma. Note also the ∼4-fold difference between old controls and old individuals with asthma [3].*

that patients with different symptoms exhale different volumes of air in the first second relative to the total volume they can exhale.

Because the FEV_1 is measured following the application of a broncho-dilator, it is essentially an indication of airway remodelling, not an indication of airway hyper-responsiveness. Hence, although ASM mass increase leads both to a permanent decrease in airway lumen size and to an increase in ASM contractility (hyper-responsiveness), we focus in this study group on the permanent effect of ASM increase in lung function, since we were provided with data on FEV_1 (Figs. 4 and 5). Note also that mathematical modelling studies of airway mechanics, including the effect of ASM mass increase on contraction, have been previously carried out (e.g. [7]).

In this work, we focus on the following two goals: formulating a model for the proliferation of ASM cells *in vivo*, and investigating how the greater reduction in lung function observed in people with asthma can be explained by an increase in ASM mass. Initially, in sec. 3.1.1, we assume that all ASM cells are proliferative and proliferate exponentially. This is shown to be unrealistic as it would lead to airway closure in a very small amount of time. Taking into account the presence of non-proliferative ASM cells as well as the ability for proliferative cells to become non-proliferative, it is found that bounded growth can occur. In sec. 3.1.2, we consider logistic growth instead of exponential growth, as it is more realistic. Initially, only switching from the proliferative to the non-proliferative pool is allowed in the model. Although changing the sole rate of proliferation produces realistic differences in cell number between healthy people and people with asthma, we are unable to obtain monotonic growth with this model. Therefore, the transition from non-proliferative to proliferative is introduced, and is shown to allow monotonic growth. In sec. 3.1.3, asymptotic analysis is used to determine the relative orders of magnitude that must characterise the rate parameters in

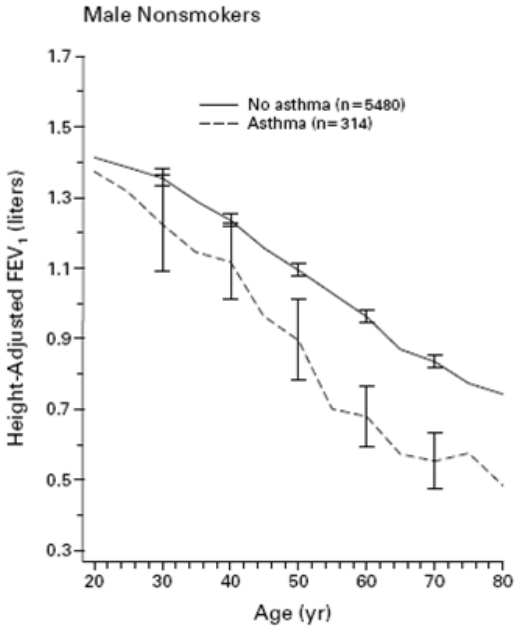

Figure 4. *Graph showing the natural decline in FEV_1 in healthy individuals and the more rapid decline in people with asthma [25].*

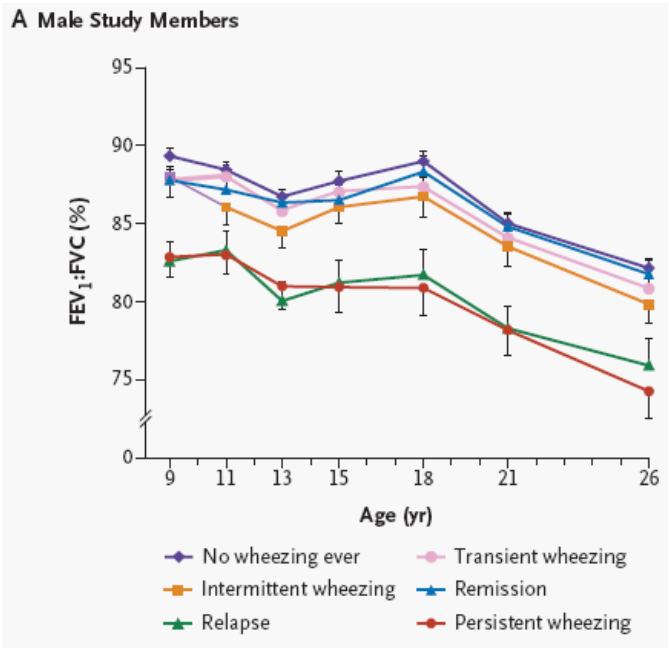

Figure 5. *Graph showing the differences in lung function, depending on what asthma symptoms are exhibited [29]. FEV_1/FVC is the FEV_1 reading divided by the total volume exhaled (FVC=forced vital capacity).*

order to obtain realistic growth over the long term. Sec. 3.2 considers how mathematical modelling may be used to relate a decrease in airway calibre (e.g., due to ASM mass increase) to a decrease in lung function. A brief introduction to general lung mechanics is given, before the theory of Poiseuille flow is described. Poiseuille flow is used as a first approximation, however it is shown that the assumptions conditioning its validity (steady laminar flow) do not hold in large airways. Incorporating corrections for turbulent flow, a more general model is presented. Finally, in sec. 4, our findings from sec. 3 are discussed. The key observations are highlighted and areas for further mathematical modelling and additional biological experiments are suggested.

3 Mathematical modelling

3.1 Population model for ASM cells proliferation and apoptosis

3.1.1 Exponential growth

The first objective of the challenge was to quantify how unrealistic it would be to use the *in vitro* cell proliferation rate as an estimate of the *in vivo* proliferation rates. Indeed, the number of ASM cells has been observed to increase by a factor of 3.24 over a 48 hour period in culture (C. Billington, unpublished work), which seems like an enormous rate if it was to apply constantly *in vivo*, and would certainly lead to airway occlusion in an implausibly small amount of time. To quantify this, we consider an intermediate sized airway with radius 0.5mm, surrounded by a layer of ASM 0.036mm thick [22]. Supposing that half the increase in ASM mass is directed inwards, reducing the airway calibre, while the other half is directed outwards, and assuming that all the cells have a similar size, then the time taken for the intermediate airway to become completely blocked with ASM is t hours, where t satisfies

$$0.018 \times 3.24^{t/48} = 0.5. \tag{1}$$

Evaluating this expression, we find that $t \sim 136$hours, which is less than six days, so clearly ASM cells cannot proliferate *in vivo* at the *in vitro* proliferation rate on the basis of an exponential growth. We note that the assumptions made in this calculation are very soft, the circular geometry of the airway is not taken into account, if this correction was made, the airway would close even faster. Also, the reduction in airway calibre is likely to impact on the FEV_1, long before the airway is completely closed. Despite being a very crude calculation, we feel it is illustrative of the fact that the remodelling of ASM associated with chronic asthma cannot be due to all the ASM cells in the lungs of asthmatic patients proliferating with a constant rate equal to the observed *in vitro* proliferation rate.

A second hypothesis we were asked to consider is to assume that the fast *in vitro* proliferation rate is applicable to a fraction of the ASM cells only, since in culture, the fastest proliferating cells tend to be selected upon passaging. Under the same assumptions as above, with a proportion k of the initial cell population proliferating at the *in vitro* rate and the remainder being non-proliferative, and assuming that daughter cells proliferate at the same rate that their parent cell does, then the time taken to block our example 0.5mm radius airway is

$$0.018k \times 3.24^{t/48} = 0.5. \tag{2}$$

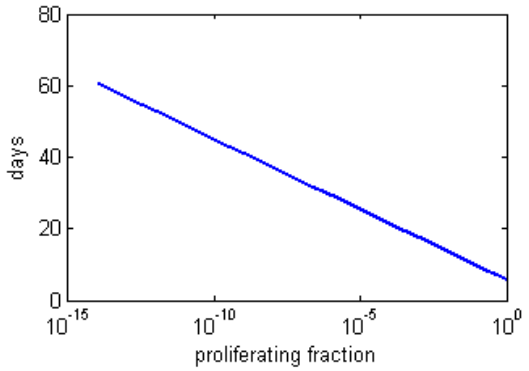

Figure 6. *Graph showing the time to airway closure in days as a function of the initial fraction of cells that proliferate at the in vitro rate. Note that the human body has of the order* 10^{13} *cells [28].*

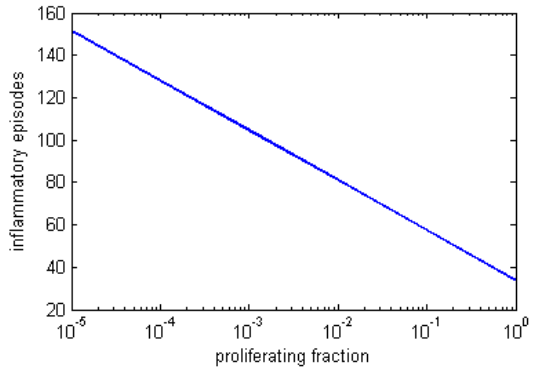

Figure 7. *Graph showing the number of attacks to airway closure as a function of the initial fraction of cells that proliferate at the in vitro rate.*

Figure 6 shows the number of days to closure as a function of the initial fraction of proliferating cells. This indicates that the *in vitro* proliferation rate cannot be applied to even a small proportion of ASM cells in the lungs if proliferation rates are simply inherited, because the proliferative population soon dominates.

A third situation we were asked to analyse is how hyperplasia occurs if ASM cells are assumed to proliferate at the *in vitro* proliferation rate, but only during short periods of time corresponding to asthma attacks. Indeed, asthma attacks are inflammatory episodes, and these are known to stimulate proliferation through the production of cytokines and growth factors (e.g., [16]), so that it is plausible that proliferation could be restricted to these episodes. To investigate this hypothesis, we assumed that an asthma attack triggers four hours of proliferation and computed the number of attacks required to close our example airway as a function of the fraction of proliferative cells in the initial population. The result is shown in Figure 7. The number of attacks before closure is not completely unreasonable, so our rough calculation has highlighted intermittent bursts of proliferation as a mechanism to further investigate.

It should be noted however, that such an intermittent growth for a single proliferative

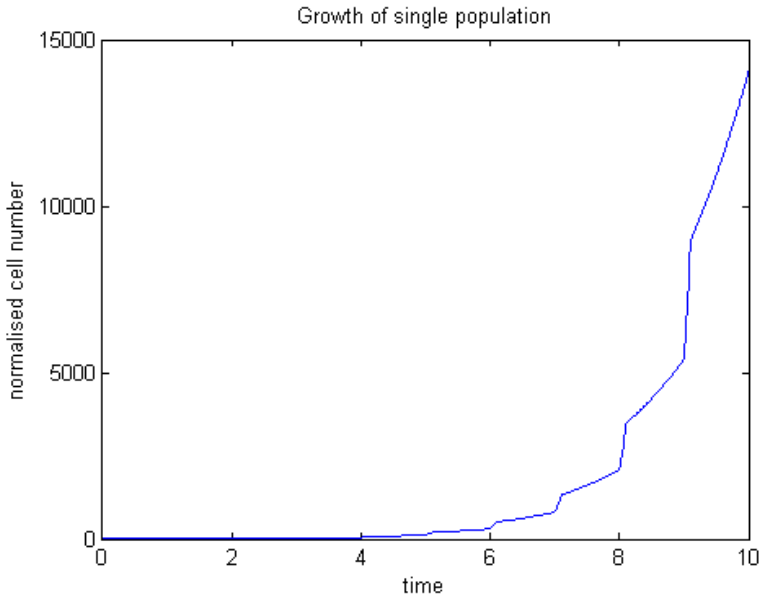

Figure 8. *Exponential growth for the single population model with intermittent growth given by equations* (3) *with* $\lambda_{\min} = 0.5$, $\lambda_{\max} = 5$, $\tau = 0.1$

population remains exponential. Consider the system:

$$\frac{dp}{dt} = \lambda(t)p(t) \tag{3a}$$

$$\lambda(t) = \lambda_{\min}(1 - \sigma(t)) + \lambda_{\max}\sigma(t) \tag{3b}$$

$$\sigma(t) = \begin{cases} 1 & 0 \leq t - n \leq \tau \qquad \text{for } n \in \mathbb{Z} \\ 0 & \text{otherwise} \end{cases} \tag{3c}$$

The solution can easily be computed:

$$p(T) = p(0)e^{(\lambda_{min}(1-\tau)+\lambda_{max}\tau)T} \qquad \text{for } T \in \mathbb{Z} \tag{4}$$

An example is illustrated in figure 8.

Let us now examine what happens if we consider the biologically more realistic hypothesis of two populations of cells, proliferative and non-proliferative, with the proliferative cells being able to turn non-proliferative. Equations (5) update model (3) with this assumption, introducing a parameter, λ_{pc} giving the transition rate from proliferative (p) to non-proliferative (c).

$$\frac{dp}{dt} = (\lambda(t) - \lambda_{pc})p(t) \tag{5a}$$
$$\frac{dc}{dt} = \lambda_{pc}p(t) \tag{5b}$$
$$\lambda(t) = \lambda_{\min}(1 - \sigma(t)) + \lambda_{\max}\sigma(t) \tag{5c}$$
$$\sigma(t) = \begin{cases} 1 & 0 \leq t - n \leq \tau \qquad \text{for } n \in \mathbb{Z} \\ 0 & \text{otherwise} \end{cases} \tag{5d}$$

Again, we can solve this model exactly, and show that in this case, the overall population growth need not be exponential (neither increasing nor decreasing). Indeed, for a given integer, n, we have

$$\begin{aligned} p(n+\tau) &= e^{(\lambda_{\max}-\lambda_{pc})\tau}p(n) \\ p(n+1) &= e^{(\lambda_{\min}-\lambda_{pc})(1-\tau)}p(n+\tau) \\ &= e^{\tau\lambda_{\max}+(1-\tau)\lambda_{\min}-\lambda_{pc}}p(n) \\ &= e^{n(\tau\lambda_{\max}+(1-\tau)\lambda_{\min}-\lambda_{pc})}p(0) \end{aligned}$$

Clearly p still behaves exponentially. For convenience, define the homogenised growth rate to be $\lambda_{hom} := (\tau\lambda_{\max} + (1-\tau)\lambda_{\min})$, so

$$p(n) = e^{n(\lambda_{hom}-\lambda_{pc})}p(0). \tag{6}$$

If $\lambda_{hom} - \lambda_{pc} < 0$, p decays (or remains constant), in which case, the asymptotic behaviour of c is not exponential:

$$\begin{aligned} c(n+\tau) &= c(n) + \frac{\lambda_{pc}}{\lambda_{\max} - \lambda_{pc}}(e^{(\lambda_{\max}-\lambda_{pc})\tau} - 1)p(n) \\ c(n+1) &= c(n+\tau) + \frac{\lambda_{pc}}{\lambda_{\min} - \lambda_{pc}}(e^{(\lambda_{\min}-\lambda_{pc})(1-\tau)} - 1)p(n+\tau) \\ &= c(n+\tau) + \frac{\lambda_{pc}}{\lambda_{\min} - \lambda_{pc}}(e^{(\lambda_{hom}-\lambda_{pc})} - e^{\tau(\lambda_{\max}-\lambda_{pc})})p(n) \\ &= c(n) + \gamma p(n) \end{aligned}$$

where

$$\gamma = \lambda_{pc}\left(\frac{e^{\tau(\lambda_{\max}-\lambda_{pc})} - 1}{\lambda_{\max} - \lambda_{pc}} + \frac{e^{\tau(\lambda_{\max}-\lambda_{pc})} - e^{(\lambda_{hom}-\lambda_{pc})}}{\lambda_{pc} - \lambda_{\min}}\right)$$

Hence

$$c(n) = c(0) + \gamma p(0)\frac{1 - e^{n(\lambda_{hom}-\lambda_{pc})}}{1 - e^{(\lambda_{hom}-\lambda_{pc})}} \tag{7}$$

Equations (6) and (7) show that the dynamics of the model are purely determined by $\lambda_{hom} - \lambda_{pc}$, with γ acting as a scaling factor. In particular, for $n \ll 1/(\lambda_{hom} - \lambda_{pc})$, we have the linear behaviour,

$$c \sim c(0) + \frac{\gamma p(0)(\lambda_{hom} - \lambda_{pc})}{1 - e^{(\lambda_{hom}-\lambda_{pc})}}n,$$

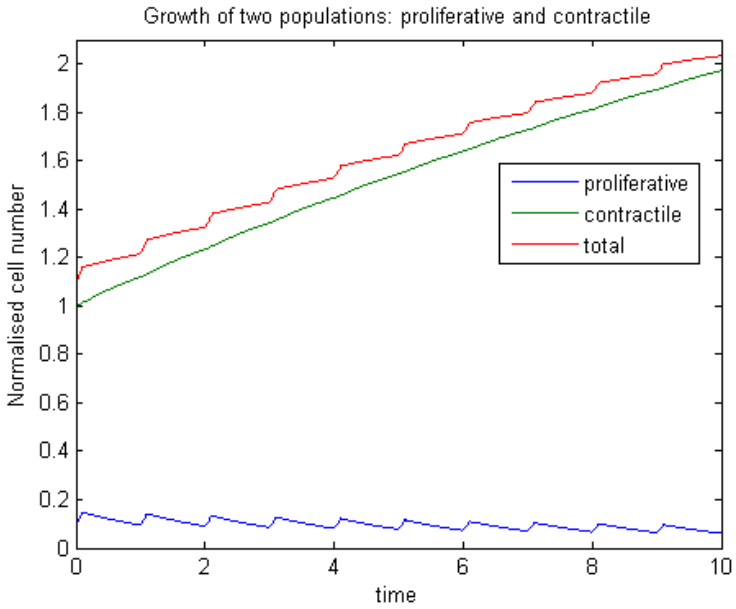

Figure 9. *Short-term dynamics for the 2 population model with intermittent growth-rates given by equations* (5) *with* $\lambda_{\min} = 0.5$, $\lambda_{\max} = 5$, $\tau = 0.1$ *and* $\lambda_{pc} = 1$, *showing almost linear growth.The proportion of proliferating cells is assumed to be small initially since it is only a few percents in healthy persons [18].*

and in the limit $n \to \infty$,

$$c \to c(0) + \frac{\gamma p(0)}{1 - e^{(\lambda_{hom} - \lambda_{pc})}}.$$

The short-term and long-term behaviors are illustrated respectively in figures 9 and 10.

Note that in the special case, $(\lambda_{hom} - \lambda_{pc}) = 0$, where the population of p is stable, $c(n) = \gamma n$, which is linear for all time, although this requires a fine balance between the λs.

Some further analysis is necessary to see whether:

- It is possible to account for both healthy and diseased cases with this model using a single parameter change.
- All intermittent models can be reduced to a non-intermittent model via a suitable choice of λ_{hom} and λ_{pc}.

Note that this second question (to which the answer seems likely to be 'yes') suggests that intermittency is something of a red-herring, dynamically speaking.

3.1.2 Logistic growth

Although we have seen that two-population models can exhibit linear growth regimes and fail to explode exponentially if proliferating cells can turn non-proliferative, this behaviour requires an exponential decay of the proliferative cell population. There is no biological evidence for this (rather, the proportion of proliferating cells can reach as much as 36% in severe asthma [18]), so it makes sense to look for models that allow the

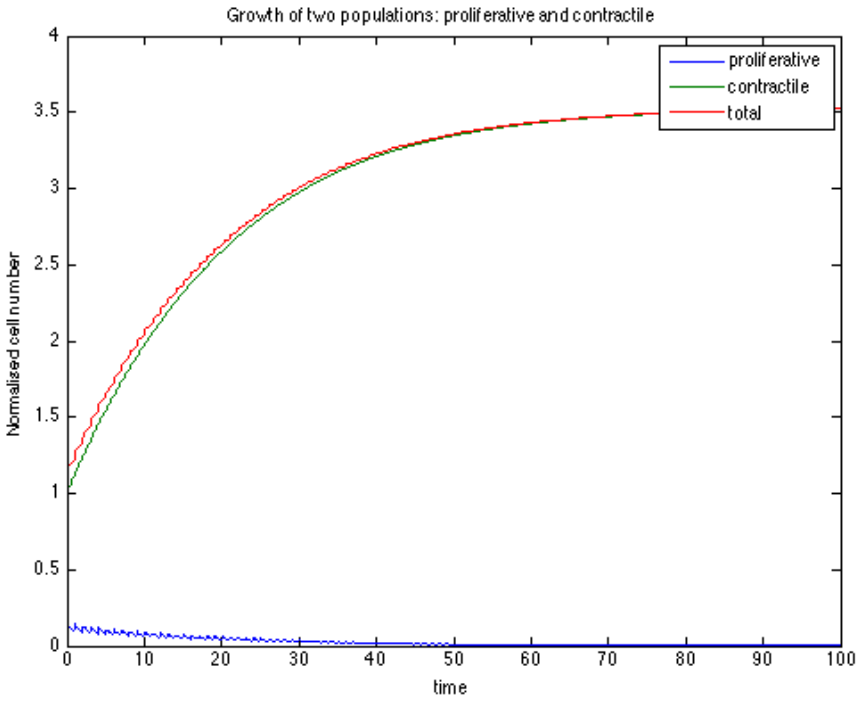

Figure 10. *Long-term dynamics for the 2 population model given by equations* (5) *with* $\lambda_{\min} = 0.5$, $\lambda_{\max} = 5$, $\tau = 0.1$ *and* $\lambda_{pc} = 1$.

proliferating population to persist. We might instead expect ASM growth to be limited by the available space and cell-contact inhibition.

We can incorporate this behaviour by proposing that cells proliferate *in vivo* according to a logistic law. Logistic growth for a population s is characterized by a "growth rate" λ and a "carrying capacity" V:

$$\dot{s} = \lambda s(1 - \frac{s}{V}) \tag{8}$$

The carrying capacity V accounts for the fact that the population is bounded from above. In this single-population model, V is the only stable steady-state ($s = 0$ is another steady-state, but it is unstable).

As above, we consider a two-population model, in which only one population can proliferate, and in which proliferating cells can turn non-proliferative. The reverse transition (non-proliferative $\rightarrow$ proliferative) is believed to occur at a negligible rate (I. Hall, personal communication), so we neglect it in the first stage. We also assume that cells can die, although with a small apoptosis rate, since apoptotic cells are hardly found in biopsies from asthmatic patients (S. Johnson, personal communication). In contrast with (5), we assume that the rate parameters are constant over time. We therefore have (see also Fig. 13):

$$\begin{aligned} \frac{dp}{dt} =& \lambda_p p \left(1 - \frac{p+c}{V}\right) - \lambda_{pc} p \\ \frac{dc}{dt} =& \lambda_{pc} p - \lambda_a c \end{aligned} \tag{9}$$

where p denotes proliferating cells and c non-proliferating cells, and where λ_a denotes the apoptosis rate. We do not include explicitly an apoptosis term for the proliferative cells as it can be absorbed into the carrying capacity V without loss of generality. A non-trivial steady-state exists if $\lambda_a \neq 0$, and is then given by:

$$\begin{aligned} p_e =& \frac{1 - \frac{\lambda_{pc}}{\lambda_p}}{1 + \frac{\lambda_{pc}}{\lambda_a}} V \\ c_e =& \frac{\lambda_{pc}}{\lambda_a} p \end{aligned} \tag{10}$$

so that the total "number" of cells at equilibrium is

$$s_e = p_e + c_e = \left(1 - \frac{\lambda_{pc}}{\lambda_p}\right) V \equiv V_{eff}. \tag{11}$$

For these quantities to be positive, we have the requirement

$$\frac{\lambda_{pc}}{\lambda_p} < 1.$$

Computation of the trace and determinant of the Jacobian shows that the non-trivial steady-state is stable provided that $V_{eff} > 0$, which holds from above.

It is interesting to note that the effect of the coupling term $\lambda_{pc} p$ is to make the "effective" carrying capacity V_{eff} depend on the growth rate λ_p. This makes it conceivable to account for the transition healthy $\rightarrow$ people with asthma in Figure 3 by tuning only

one parameter in the model, namely λ_p, as it not only changes the rate at which the equilibrium is reached, but also the equilibrium itself (in contrast to what happens in the single-population model). However, as increasing λ_p is necessary to make the carrying capacity larger, it implies that for a range of initial conditions, the people with asthma will reach steady-state before the healthy, which may not be satisfying from a conceptual point of view.

However, there is a more important problem. Let us assume that a healthy person turns asthmatics via a permanent increase in λ_p from λ_{ph} to λ_{pa}, and let us consider the following non-dimensionalisation for facility: $p^* = p/V$, $c^* = c/V$, and $t^* = \lambda_{pc}t$. We also define $\lambda_p^* = \lambda_p/\lambda_{pc}$, and $\lambda_a^* = \lambda_a/\lambda_{pc}$. Droping immediately the *, we have:

$$\begin{aligned} \frac{dp}{dt} =& \lambda_p p\,(1-p-c) - p \\ \frac{dc}{dt} =& p - \lambda_a c \end{aligned} \tag{12}$$

so that the non-trivial steady-state is given by:

$$\begin{aligned} p_e =& \frac{1-\frac{1}{\lambda_p}}{1+\frac{1}{\lambda_a}} \\ c_e =& \frac{p}{\lambda_a} \end{aligned} \tag{13}$$

and

$$s_e = p_e + c_e = 1 - \frac{1}{\lambda_p} \tag{14}$$

giving rise to the condition $\lambda_p > 1$.

We can now calculate easily the value of λ_{pa} necessary to have a 4-fold difference in ASM mass between healthy and people with asthma at steady-state, in agreement with the experimental data from Figure 3, from the relation:

$$1 - \frac{1}{\lambda_{pa}} = 4\left(1 - \frac{1}{\lambda_{ph}}\right).$$

This gives

$$\lambda_{pa} = \frac{\lambda_{ph}}{4 - 3\lambda_{ph}} \tag{15}$$

together with the condition $\lambda_{ph} < 4/3$.

If we now simulate the model with $\lambda_p = \lambda_{pa}$ given by (15), starting from an initial condition such that s is half its steady-state value for $\lambda_p = \lambda_{ph}$, with some $\lambda_{ph} \in (1, 4/3)$, and $\lambda_a \ll 1$, we observe that the total cell population s exhibits oscillations of decreasing amplitude before becoming constant (Fig. 11). This implies that the ASM mass of people with asthma would decrease in some periods of their life, which is counter-intuitive and has not been reported. We can actually prove that these transient oscillations are unavoidable in this model for $\lambda_a \ll 1$, as the steady-state is a focus if

$$\tau^2 - 4\Delta = \lambda_a^2\left(\frac{\lambda_p + \lambda_a}{1+\lambda_a}\right)^2 - 4\lambda_a(\lambda_p - 1) < 0, \tag{16}$$

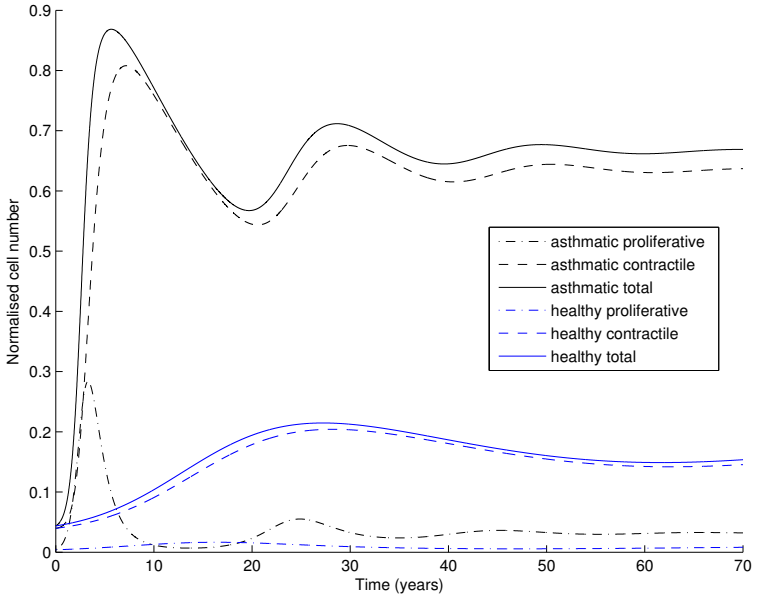

Figure 11. *Numerical solution to* (12) *with* $\lambda_{ph} = 1.2$ *(*$\Rightarrow \lambda_{pa} = 3$*), and* $\lambda_a = 0.05$.

where τ (resp. Δ) is the trace (resp. the determinant) of the Jacobian evaluated at the steady-state. This condition is always satisfied if $\lambda_a \ll 1$, since

$$\tau^2 - 4\Delta \simeq -4\lambda_a(\lambda_p - 1) + O(\lambda_a^2). \tag{17}$$

This observation lead us to re-incorporate in the model the possibility for the non-proliferative population to turn proliferative:

$$\begin{aligned} \frac{dp}{dt} =& \lambda_p p\,(1 - p - c) - p + \lambda_{cp} c \\ \frac{dc}{dt} =& p - \lambda_a c - \lambda_{cp} c \end{aligned} \tag{18}$$

for which the non-trivial steady-state is given by:

$$s_e = \frac{\lambda_{cp} + \left(1 - \frac{1}{\lambda_p}\right)\lambda_a}{\lambda_{cp} + \lambda_{cp}}. \tag{19}$$

It is positive if

$$\lambda_p > \frac{\lambda_a}{\lambda_a + \lambda_{cp}}.$$

As above, we can work out the condition for a 4-fold increase in ASM cell equilibrium population when we change λ_p from λ_{ph} to λ_{pa}:

$$-3\lambda_{ph}\left(1 + \frac{\lambda_{cp}}{\lambda_a}\right) + 4 > 0 \tag{20}$$

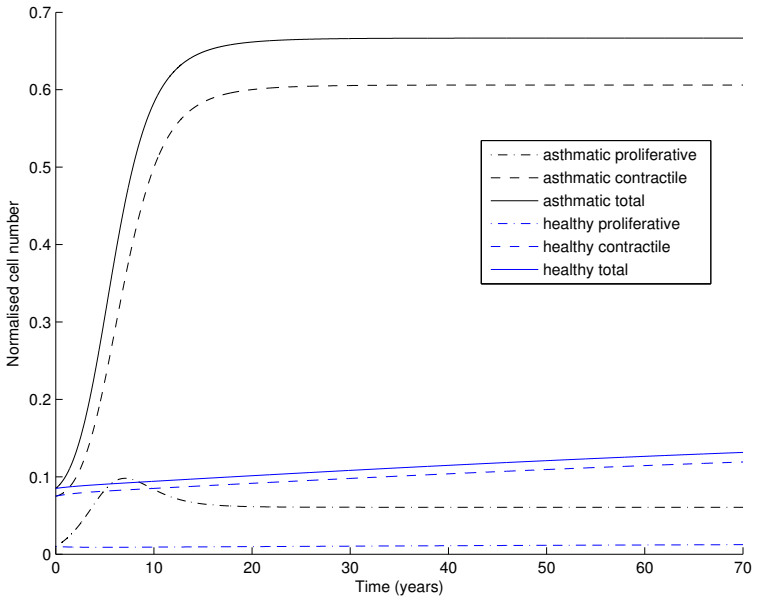

Figure 12. *Numerical solution to* (18) *with* $\lambda_{ph} = 0.6$ *(*$\Rightarrow \lambda_{pa} = 1.5$*),* $\lambda_a = 0.05$*, and* $\lambda_{cp} = 0.05$.

in which case $\lambda_{pa} = \frac{1}{1-\alpha}$ where

$$\alpha = 3\frac{\lambda_{cp}}{\lambda_a} + 4\left(\frac{\lambda_{ph} - 1}{\lambda_{ph}}\right). \tag{21}$$

With this extended model, we were able to obtain a monotonic behaviour for the total cell population (Fig. 12). The progression of the healthy toward steady-state is still slower than that of people with asthma, but it is monotonic as well. Further analysis of this model is left for future work.

In the next section, we consider an alternative mechanism for ASM mass increase in asthma: namely, that the transition rate λ_{cp} exhibits spike increases during asthma attacks, while the growth rate λ_p remains unchanged ($\lambda_{pa} = \lambda_{ph}$).

3.1.3 Two-timescale analysis of ASM logistic population dynamics with exacerbation events

In this section we consider the effect of varying the $c \to p$ switching rate (λ_{cp}), mimicking the exacerbation events, on both the short-term and long-term population growth.

Consider the following system of ODEs, describing the two-populations dynamics represented in Fig. 13, which is a dimensional version of (18) :

$$\dot{p}^* = \lambda_p\, p^* \left(1 - \frac{p^* + c^*}{V}\right) - \lambda_{pc}\, p^* + \lambda_{cp}\, c^*, \tag{22a}$$

$$\dot{c}^* = \lambda_{pc}\, p^* - (\lambda_{cp} + \lambda_a)\, c^*, \tag{22b}$$

where λ_p is the proliferation rate, λ_a is the apoptosis rate, and λ_{cp}, λ_{cp} are the switching rates, and V is the maximal total population size. The system (22) is subject to the

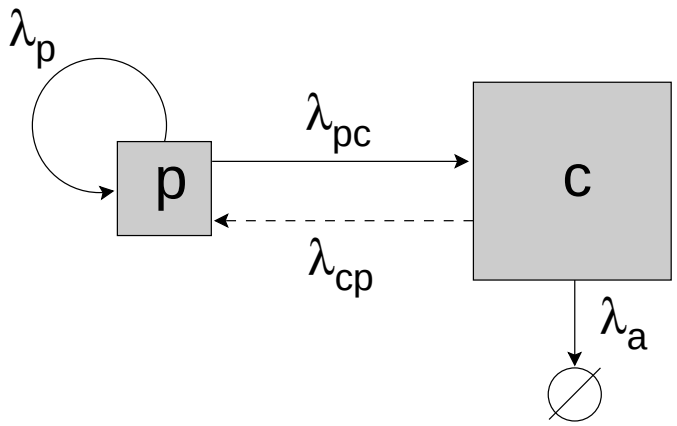

Figure 13. *Two-population dynamics diagram for contractile (c) and proliferative (p) states/sub-populations of airway-smooth-muscle cells; λ_p is the proliferation rate, λ_a is the apoptosis rate, and λ_{cp}, λ_{cp} are the switching rates.*

initial conditions $p^*|_{t*=0} = p_0^*$ and $c^*|_{t*=0} = c_0^*$. The total ASM population is

$$s^* = p^* + c^* \,. \tag{23}$$

We choose the dimensionless variables $c^* = V\,c,\ p^* = \varepsilon\,V\,p,\ s^* = V\,s,\ t^* = t/\lambda_p$, (instead of $t^* = t/\lambda_{pc}$ as above) and we assume the following:

- The initial (sub)population of rapidly proliferating cells is small: $\varepsilon = \frac{p_0^*}{c_0^*} \ll 1$;
- The $p \to c$ switching occurs more often than the cell proliferation: $\frac{\lambda_{pc}}{\lambda_p} = O(\varepsilon^{-1}) = \nu_{pc}\,\varepsilon^{-1}$;
- The $c \to p$ switching happens in a periodic series of events ("spikes") separated by an average period τ (in dimensionless variables): $\frac{\lambda_{cp}}{\lambda_p} = \nu_{cp}\,[\varepsilon + \sum_{n=0}^{\infty} \delta(t - n\,\tau)]$;
- We neglect apoptosis for the p-population (which is partially accounted for in the logistic law), and we assume the apoptosis for the c-population is much slower than the baseline $c \to p$ switching: $\frac{\lambda_a}{\lambda_p} = O(\varepsilon^2) = \nu_a\,\varepsilon^2$.

Here $\nu_{pc},\ \nu_{cp},\ \nu_a$ and τ are dimensionless $O(1)$ parameters.

The system (22) in a non-dimensional form is

$$\varepsilon\,\dot{p} = \varepsilon\,p\,(1 - c - \varepsilon\,p) - \nu_{pc}\,p + \nu_{cp}\left[\varepsilon + \sum_{n=0}^{\infty} \delta(t - n\,\tau)\right] c\,, \tag{24a}$$

$$\dot{c} = \nu_{pc}\,p - \nu_{cp}\left[\varepsilon + \sum_{n=0}^{\infty} \delta(t - n\,\tau)\right] c - \varepsilon^2\,\nu_a\,c\,, \tag{24b}$$

and

$$s = c + \varepsilon\,p\,. \tag{25}$$

We look for solution to (24), using two-timescale functions

$$p = \tilde{p}(t, T) \quad \text{and} \quad c = \tilde{c}(t, T)\,, \quad (\,\dot{p} = \tilde{p}_t + \varepsilon\,\tilde{p}_T\,,\ \dot{c} = \tilde{c}_t + \varepsilon\,\tilde{c}_T)\ , \tag{26}$$

with a slowly varying time coordinate $T = \varepsilon\, t$ $(\varepsilon \to 0)$, and expanding into an asymptotic series with respect to ε

$$\tilde{p}(t,T) \approx p^{(0)} + \varepsilon\, p^{(1)} + \dots\,, \quad \tilde{c}(t,T) \approx c^{(0)} + \varepsilon\, c^{(1)} + \dots\,. \tag{27}$$

Substituting (26) and (27) into (24) and collecting terms at powers in ε, we get at $O(\varepsilon^0)$:

$$-\,\nu_{pc}\, p^{(0)} + \nu_{cp} \sum_{n=0}^{\infty} \delta(t - n\,\tau)\, c^{(0)} = 0\,,$$

$$c_t^{(0)} = \nu_{pc}\, p^{(0)} - \nu_{cp} \sum_{n=0}^{\infty} \delta(t - n\,\tau)\, c^{(0)}\,,$$

which simplifies to

$$p^{(0)} = \frac{\nu_{cp}}{\nu_{pc}} \sum_{n=0}^{\infty} \delta(t - n\,\tau)\, c^{(0)}\,, \tag{29a}$$

$$c^{(0)} = c^{(0)}(T)\,, \tag{29b}$$

i.e. the size of the c-population, at leading order, is independent of the fast-varying time t, and $p^{(0)}$ is a t-periodic function of period τ.

Collecting the terms at $O(\varepsilon^1)$, we get

$$p_t^{(0)} = p^{(0)}\,(1 - c^{(0)}) - \nu_{pc}\, p^{(1)} + \nu_{cp}\, c^{(0)} + \nu_{cp} \sum_{n=0}^{\infty} \delta(t - n\,\tau)\, c^{(1)}\,, \tag{30a}$$

$$c_t^{(1)} + c_T^{(0)} = \nu_{pc}\, p^{(1)} - \nu_{cp}\, c^{(0)} - \nu_{cp} \sum_{n=0}^{\infty} \delta(t - n\,\tau)\, c^{(1)}\,, \tag{30b}$$

and summing up the equations in (30), we have

$$c_T^{(0)} = p^{(0)}\,(1 - c^{(0)}) - p_t^{(0)} - c_t^{(1)}\,. \tag{31}$$

Integrating (29a) and (31) over a single period $(-\tau/2 \le t' = t - n\,\tau \le \tau/2;\ n$ is an arbitrary "exacerbation" event), we obtain

$$\langle p^{(0)} \rangle = \frac{\nu_{cp}}{\nu_{pc}\,\tau}\, c^{(0)} \int_{-\tau/2}^{\tau/2} \delta(t')\,\mathrm{d}t' = \frac{\nu_{cp}}{\nu_{pc}\,\tau}\, c^{(0)}(T)\,, \tag{32a}$$

$$c_T^{(0)} = \langle p^{(0)} \rangle\,(1 - c^{(0)}) - \frac{1}{\tau}\, p^{(0)}\Big|_{-\tau/2}^{\tau/2} - \frac{1}{\tau}\, c^{(1)}\Big|_{-\tau/2}^{\tau/2}\,, \tag{32b}$$

where $\langle f \rangle \equiv \frac{1}{\tau} \int_{-\tau/2}^{\tau/2} f\ \mathrm{d}t$. Taking into account t-periodicity of $p^{(0)}$ from (29a), assuming t-periodicity of $c^{(1)}$ (verified *a posteriori*), and substituting (32a) into (32b), we find the logistic growth of c-population at leading-order:

$$s_T^{(0)} \equiv c_T^{(0)} = \frac{\nu_{cp}}{\tau\, \nu_{pc}}\, c^{(0)}\,(1 - c^{(0)})\,, \tag{33}$$

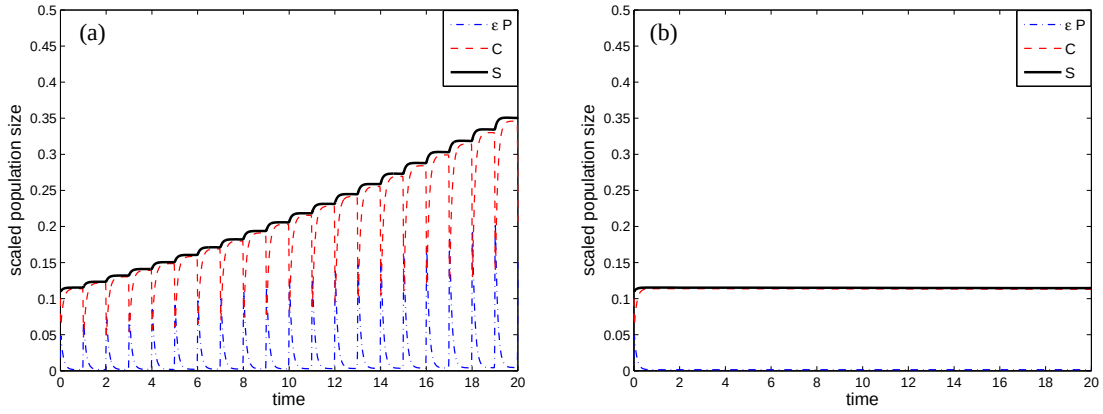

Figure 14. *Numerical solution to (24) with δ-function approximated by a Gaussian pulse $\delta(t-n\tau) \approx \exp\{-(t-n\tau)^2/(2\sigma^2)\}/\sqrt{2\pi\sigma^2}$ ($\sigma = 0.01$) for frequent exacerbation events (pathology) $\tau = 1$ (a) and no exacerbation events (control group) $\tau = 100$ (b). Plotted in dimensionless variables for $\varepsilon = 0.1$, $\nu_{pc} = 1$, $\nu_{cp} = 1.2$, $\nu_a = 1.2$, $p(0) = c(0) = 0.1$. As predicted by (33), the total population in (a) saturates in the long term (not shown).*

where relation (25) implies

$$s^{(0)} = c^{(0)}\,, \quad s^{(1)} = c^{(1)} + p^{(0)}\,. \tag{34}$$

In order to estimate the first correction, we substitute (33) into (31), and use (32a) to obtain

$$c_t^{(1)} = \left(p^{(0)} - \langle p^{(0)}\rangle\right)(1-c^{(0)}) - p_t^{(0)}\,, \tag{35}$$

which for $n\tau < t < (n+1)\tau$ (since there is no "spikes" in $p^{(0)}$ between two consequent exacerbation events, i.e. $p^{(0)} = 0$) and by use of (29a) simplifies to

$$c_t^{(1)} = -\langle p^{(0)}\rangle(1-c^{(0)}) = -\frac{\nu_{cp}}{\tau\,\nu_{pc}}\,c^{(0)}\,(1-c^{(0)})\,,$$

with $c^{(1)}|_{t=0} = 0$ to satisfy the initial condition $\tilde{c}|_{t=0} = c_0 = O(1)$, giving the correction

$$c^{(1)} = -\frac{\nu_{cp}}{\nu_{pc}}\,c^{(0)}\,(1-c^{(0)})\,\frac{t}{\tau}\,, \quad n\tau < t < (n+1)\tau\,,\ n = 0,1,\dots\,, \tag{36}$$

which is a periodic "saw-tooth" function of period τ. The correction to the total population size $s^{(1)} = c^{(1)} + p^{(0)}$ is thus given by (29a) and (36).

We therefore conclude that the periodic "spikes" in the $c \to p$ switching rate result in the scale-separation ($s \approx s^{(0)}(T) + \varepsilon\, s^{(1)}(T/\varepsilon, T)$), where rapid oscillations in the size of p-population of ASM cells $p^{(0)}$ provide a net growth in the size of c-population and the total population size $s^{(0)} = c^{(0)}$ in a longer term, which is confirmed by a direct numerical simulation in `Matlab` with `ode23t` solver (see Fig. 14a). The rate of the slow-timescale growth in (33) is proportional to the ratio of switching rates $\bar{\lambda}_{cp}/\lambda_{pc}$ (where $\bar{\lambda}_{cp} = \varepsilon\nu_{cp}$) and inversely proportional to the period between exacerbation $1/\tau^*$ (in the original dimensional variables).

Finally, we consider the case of very infrequent exacerbations ($\tau \gg 1$). In this limit, the two-population system (24) takes the following form:

$$\varepsilon\,\dot{p} = \varepsilon\,p\,(1 - c - \varepsilon\,p) - \nu_{pc}\,p + \varepsilon\,\nu_{cp}\,c\,, \tag{37a}$$

$$\dot{c} = \nu_{pc}\,p - \varepsilon\,\nu_{cp}\,c - \varepsilon^2\,\nu_a\,c\,, \tag{37b}$$

subject to the initial conditions $p|_{t=0} = p_0,\ \ c|_{t=0} = c_0$. Since there are no longer two-distinct time-scales being present, we consider the dynamics only in a slow-time coordinate $T = \varepsilon\,t$ and use expansion (27) to get from (37), at $O(\varepsilon^0)$:

$$p^{(0)} \equiv 0\,, \quad c^{(0)} = c^{(0)}(T)\,, \tag{38}$$

at $O(\varepsilon^1)$:

$$0 = -\nu_{pc}\,p^{(1)} + \nu_{cp}\,c^{(0)}\,, \tag{39a}$$

$$c_T^{(0)} = \nu_{pc}\,p^{(1)} - \nu_{cp}\,c^{(0)}\,, \tag{39b}$$

which (by summing up (39a) and (39b) reduces to

$$c^{(0)} = \text{const}\,, \quad p^{(1)} = \frac{\nu_{cp}}{\nu_{pc}}\,c^{(0)} = \text{const}\,, \tag{40}$$

and at $O(\varepsilon^2)$, (37) gives

$$0 = p^{(1)}\,(1 - c^{(0)}) - \nu_{pc}\,p^{(2)} + \nu_{cp}\,c^{(1)}\,. \tag{41a}$$

$$c_T^{(1)} = \nu_{pc}\,p^{(2)} - \nu_{cp}c^{(1)} - \nu_a\,c^{(0)}\,, \tag{41b}$$

Summing up the equations in (41), applying (40) and using the initial condition $c^{(0)}|_{t=0} \approx c_0$, we find

$$c_T^{(1)} = \frac{\nu_{cp}}{\nu_{pc}}\,c_0\,(1 - c_0) - \nu_a\,c_0\,. \tag{42}$$

Therefore, we require $\frac{\nu_{cp}}{\nu_a\,\nu_{pc}} = 1 - c_0$ in order to ensure the existence of a steady state $c_T^{(1)} = 0$ and exclude long-term ASM growth in a healthy (control) group. For small c_0, the stationarity condition is

$$\frac{\nu_{cp}}{\nu_a\,\nu_{pc}} \sim 1\,, \tag{43}$$

or, in dimensional parameters,

$$\frac{\bar{\lambda}_{cp}}{\lambda_{pc}} \sim \frac{\lambda_a}{\lambda_p}\,. \tag{44}$$

Numerical simulation shown in Figure 14(b) confirms this asymptotic relation.

3.2 ASM mass and lung function

As discussed in Section 2, the primary source of longitudinal data regarding a progressive decrease in lung function comes from the measurement of FEV_1 (the maximum volume of gas that can be expelled from the lungs during the first second following a maximal inspiration). The decline in FEV_1 with age, as reported in [25], is shown in Figure 4. The paper used a large dataset and demonstrated a significant difference between progressive

lung function decrease in healthy individuals and people with asthma. Lung function decreases as a natural consequence of aging, however this process is sped up in those with asthma; the paper states that across the subjects measured, healthy individuals demonstrated a 22 ml/year decline whilst people with asthma demonstrated a 38 ml/year decline in FEV_1 measurements [25].

This accelerated decrease in lung function is commonly attributed to airway remodelling and a major factor in this remodelling is believed to be ASM proliferation [26]. One of the main questions asked of the study group was whether or not it was possible to attribute this reduction in lung function to an increase in ASM mass. This is a complicated question as there are a number of mechanisms by which increased ASM could potentially reduce an FEV_1 measurement. At the core of the problem is the issue of flow limitation, this section shall attempt to discuss some of the key considerations and calculations.

3.2.1 General Lung Mechanics

The lung can be modelled as a branching tree of airways, often this branching is assumed to be symmetrical but it is more accurate to allow for asymmetry. In humans there may be up to 28 generations of airway, these can be broadly split into two categories—conductive airways and respiratory airways—as was done by Weibel in 1963 [33]. The conductive airways carry air into and out of the lungs, whilst the respiratory airways both carry air and participate in respiration. On a given conduit the conductive airways will extend down to between the 11th to 17th generation, known as the terminal bronchiole before the respiratory airways begin.

Decreased lung function as a result of airway remodelling in asthma could be the result of a number of factors. The first is that of increased airway resistance due to reduction in lumen cross-section, the second is that of increased lung tissue resistance to deformation such that elastic recoil during expiration is changed, finally there is the notion of airway derecruitment which occurs when air becomes trapped behind some blockage, effectively decreasing the volume of the lung (this is unlikely to have a large impact in the duration of an FEV_1 test, it would exhibit more of an effect on FVC).

Realistically it is likely that each of these factors contributes to some degree in the reduction of FEV_1 that we were asked to consider. In the time that was allotted to us we decided to focus on increased airway resistance via airway narrowing, as this seemed the mechanism that would be most affected by increases in ASM.

3.2.2 Poiseuille Flow

We began under the assumption that flow throughout most of the lung could be treated as laminar, steady flow through a pipe of constant cross-sectional area (for a given generation of airways), this is commonly known as Poiseuille flow. As we will discuss later many of these assumptions are flawed but they present a reasonable starting point. Poiseuille flow is graphically represented in figure 15(A):

As is depicted in the diagram the flow is laminar such that velocity is constant along any imaginary cylindrical path at a given radii from the centre of the pipe. The flow has zero velocity on the pipe walls at $r = a$ and reaches its maximum flow at $r = 0$. The flow is driven by the pressure gradient from P_1 to P_0. Disregarding gravitational effects and under the assumptions of steadiness, axisymmetry and non-zero velocity only in the

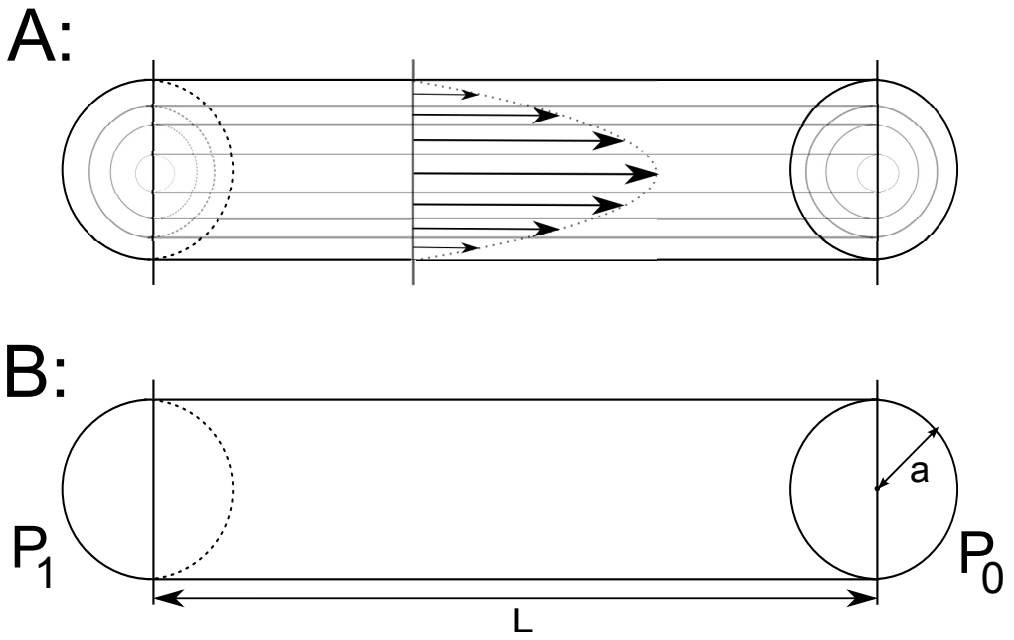

Figure 15. *Poiseuille Flow*

direction along the tube (u_z) the Navier-Stokes equations reduce to the following

$$\frac{\partial P}{\partial z} = \frac{\mu}{r}\frac{\partial}{\partial r}\left(r\frac{\partial u_z}{\partial r}\right). \tag{45}$$

Where P is the pressure in the tube and μ is the dynamic viscosity of the fluid (in this case air). This equation has the solution:

$$u_z = \frac{r^2}{4\mu}\frac{\partial P}{\partial z} + c_1 \ln r + c_2. \tag{46}$$

Such that u_z is finite at $r = 0$ we impose that $c_1 = 0$. Furthermore to satisfy the no slip condition that $u_z = 0$ at $r = a$ we set c_2 such that

$$c_2 = -\frac{a^2}{4\mu}\frac{\partial P}{\partial z}. \tag{47}$$

Then, finally we have

$$u_z = \frac{r^2 - a^2}{4\mu}\frac{\partial P}{\partial z}. \tag{48}$$

The dimensions of FEV_1 are volume over time, so it is a flux. The FEV_1 is equivalent to a flux Q, through a cylindrical pipe with radius a, which can be calculated by integrating the velocity u_z over the cross-sectional area of the pipe. In cylindrical coordinates this gives

$$Q = \int_0^a \int_0^{2\pi} u_z r \, d\theta dr \tag{49}$$

$$Q = -\frac{\pi a^4}{8\mu}\frac{\partial P}{\partial z} \tag{50}$$

Of important note from the above equation is that flux Q is proportional to airway radius a to the power 4, hence for a given pressure gradient even a small change in the diameter of the pipe (in this case lumen constriction via ASM proliferation) can lead to a large change in airflow.

3.2.3 Turbulence

The Poiseuille flow approximation relies on the assumption of steady laminar flow. Flow travelling fast enough through a pipe is liable to become turbulent (as was famously demonstrated by Osbourne Reynolds in the 19th century) and therefore violate our previous assumption of steady flow. Determination of whether flow at a given speed is turbulent or not is governed in large part by that flow's Reynolds number Re which is calculated here as

$$Re = \frac{2\rho Q}{\pi \mu a}, \tag{51}$$

where ρ represents the density of the fluid and μ represents its dynamic viscosity. In the case of air $\rho = 1.2 \times 10^{-3} g.ml^{-1}$ and $\mu = 2 \times 10^{-4} g.cm^{-1}.s^{-1}$. For an FEV_1 we expect that flow or flux will be such that Q is between 1.5 and $5.5 l.s^{-1}$ depending upon the age, height and gender of the individual. Given that it has a radius of around 1 cm, we can therefore calculate the Reynolds number in the trachea to be between $Re = 6000$ and $Re = 21000$ depending upon the FEV_1 measurement achieved. In either case this is firmly within the turbulent regime, hence violating the assumptions of Poiseuille flow.

If we take the assumption that the lung is a symmetrical, branching tree of airways such that the number of airways is equal to 2^n at generation n with $n = 0$ representing the trachea, then Poiseuille flow will still hold in the lower airways. For instance at the tenth generation, $n = 9$, we would have 512 parallel airways of radius $0.08cm$, if we divide the flux between them the Reynolds number would be around $Re = 140$ to $Re = 500$ which will usually fall within the laminar regime. As a general rule of thumb Re much greater than 2000 is likely to be turbulent and Re much less than 2000 is likely to be laminar.

3.2.4 General Model

As in [5] we shall assume that for a given lung structure, such that the airway radii and the age of the individual are fixed, the flux through the system (FEV_1) is proportional only to the pressure gradient exerted between the distal airways and the end of the airway (ΔP) such that

$$\Delta P = R_{aw}(r) Q. \tag{52}$$

Note that for the sake of ease we shall assume that this pressure remains constant for the duration of the FEV_1 measurement, however this is unlikely to hold in reality. $R_{aw}(r)$ is the airway resistance that is related to the set of radii parameters for each of the airway generations. Broadly we now aim to sum the resistance of each of the airways to obtain a total airway resistance across the lung. In the lower airways where the flow can be treated as Poiseuille we have shown by (50) that, when integrated along the length L of the conduit, that the airway resistence is equal to

$$R_p = \frac{8\mu L}{\pi a^4}. \tag{53}$$

In the case of turbulent flow we shall adopt the experimentally derived correction discussed in [31] such that we have

$$R_n = \begin{cases} R_p\left(0.556 + 0.067\sqrt{Re}\right) & \text{if } Re \geq 55 \\ R_p & \text{if } Re \leq 55, \end{cases} \tag{54}$$

where R_n is the resistance of individual airways at generation n. We now also adopt the parameter ξ as is done in paper [11], this is a scaled parameter describing the generation or length 'down' the lung ranging from $\xi = 0$ representing roughly the middle of the tenth generation of airways up to $\xi = 1$ the mid-trachea. The full length over which ξ extends is therefore roughly 18.357 cm. In the paper they also derived equations and parameters for the number of airways at a given ξ and the radius of a single (healthy) airway at the same position

$$N(\xi) = 1.038(\xi + 0.01)^{-1.36}, \tag{55}$$

$$r(\xi) = 0.8315(\xi + 0.01)^{0.53}. \tag{56}$$

If we now define ξ_c to be the critical point at which $Re = 55$, then using (51) we can calculate this to be

$$\xi_c = 20.823Q^{-1.2048} - 0.01. \tag{57}$$

Hence even for a relatively slow flow the turbulence correction will be applied across all airways above the tenth generation. Regardless we can write the total lung resistance (R_{Tot}) as

$$R_{Tot} = 18.357\left(\int_0^{\xi_c} \frac{R_p}{N(\xi)}d\xi + \int_{\xi_c}^{1} \frac{R_p\left(0.556 + 0.067\sqrt{Re}\right)}{N(\xi)}d\xi\right). \tag{58}$$

Together with (52) we can use this to find a pressure for a given flow or FEV_1. For instance we can calculate that generating a flow of $2\,\text{L.s}^{-1}$ would require a pressure of around $410\,\text{g.cm}^{-2}$ or 40.2 KPa.

3.2.5 Example of applying the general model to airway remodelling

Airway narrowing can clearly be represented by modifying the function $r(\xi)$, unfortunately we have little basis to determine how this function should be changed. To present a simple example here, however, we shall run briefly through the case where all of the airways have their radii reduced by some percentage α, such that

$$r(\xi, \alpha) = (1 - \alpha)0.8315(\xi + 0.01)^{0.53}. \tag{59}$$

We need specific flows to perform the calculation; we know that age related effects will naturally reduce FEV_1 by 22 ml/year from paper [25], additionally the paper states that the people with asthma exhibit a decline of 38 ml/year. If we accept this linear decline then we can proceed by setting the subject of our example to be an individual who's peak flow begins at $4L.s^{-1}$ and then declines in keeping with the paper's findings. Calculating the required reduction of radius to produce this effect leads to Figure 16.

This graph demonstrates that over long time scales the reduction in radius would follow a quartic decline. This implies that a larger change in radius is required to

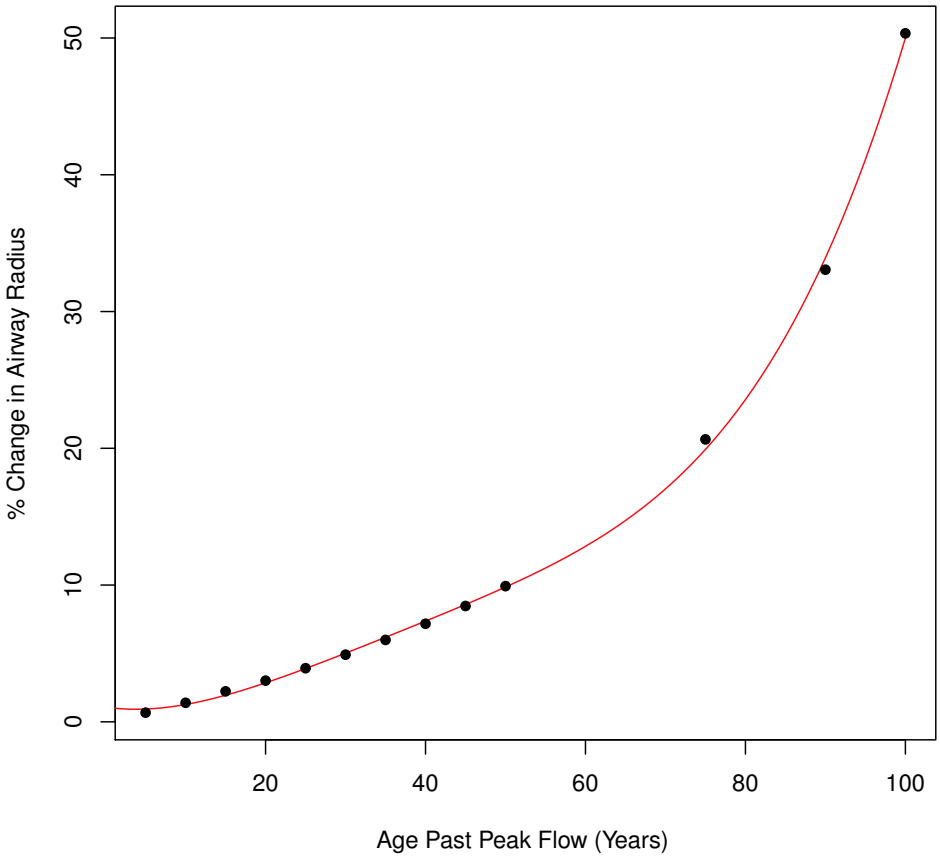

Figure 16. *Change in airway radius*

produce the same change in flow at lower starting flows. Given, however, that the ages are measured in years from peak flow (typically when individuals are in their twenties), we can expect a reasonable time course would extend over no more than 50 years, that being the case the reduction in radius is roughly linear - a reduction of 0.2% from original radius per year.

4 Discussion and Perspectives

4.1 Population growth model for ASM cells

Section 3.1 showed that a two-population model with the ability for proliferating cells to become non-proliferative is necessary to account for ASM mass increase in asthma. More precisely, it was shown in section 3.1.1 that it is possible to have the total population saturates in the long term even if the proliferative cells proliferate exponentially, provided that the switching rate is larger then the average proliferating rate. However, this implies an exponential decay of the proliferative cell population, which has not been reported experimentally. Also, it is unclear whether it is possible to explain the difference between

healthy individuals and individual with asthma by varying a single parameter in this model.

If proliferative cells are not to die out, then bounded growth (e.g., logistic growth) is also necessary. In section 3.1.2, we have studied whether a permanent increase in the logistic growth rate of the proliferative cells λ_p could explain the increase in ASM mass observed in people with asthma (Fig. 3, reproduced from [3]). We have shown that if the non-proliferative cells are unable to become proliferative (transition $c \to p$ forbidden), the model with time-invariant rates is not able to account for a monotonic increase of the total cell population, at least if the apoptosis rate is small. Instead, the ASM cell population exhibits damped oscillations toward steady-state (Fig. 11), which would imply that the ASM mass of people with asthma decreases in certain periods of their life, in contrast to what is expected. Allowing the transition $c \to p$ in the model permits to recover a monotonic behavior for the total cell mass increase, however it seems that this behavior is restricted to very small ranges of parameter values (preliminary results to be confirmed).

In Section 3.1.3, a different hypothesis was considered: we investigated the effect of repeated spike increases in the switching rate λ_{cp} ($c \to p$ transition) on ASM cell population evolution, with the logistic growth rate λ_p kept constant. This models the possibility that a substantial amount of non-proliferative cells could change phenotype and becoming proliferative during asthma attacks, while this event would be rare outside of exacerbation periods. A two-timescale analysis, assuming that 1) the initial subpopulation of proliferating cells is small, 2) the $p \to c$ switching rate λ_{pc} is large compared to the proliferation rate λ_p, 3) the basal $c \to p$ switching rate $\bar{\lambda}_{cp}$ is small compared to λ_p, and 4) the apoptosis rate λ_a is itself smaller than $\bar{\lambda}_{cp}$, , shows that periodic increases in the $c \to p$ switching rate can account for an increase in total cell population which is slow compared to the period of the exacerbation events, and which is monotonic (and more precisely, logistic) at leading order on the long timescale, in agreement with the experimental observations. The rate of the logistic increase is predicted to be proportional to the ratio $\frac{\bar{\lambda}_{cp}}{\lambda_{pc}}$ and inversely proportional to the period of the exacerbation events. In addition, the analysis shows that if the frequency of the exacerbation events is very small (which can be considered as the healthy situation), the evolution is steady at first order if $\frac{\bar{\lambda}_{cp}}{\lambda_{pc}} \sim \frac{\lambda_a}{\lambda_p}$. Therefore, this analysis provides a possible answer to the challenge question "to what extent do proliferation and apoptosis participate in the turnover rates of human ASM cells in normal and diseased tissue?". Indeed, it gives the relative orders of magnitude that must characterise the model rate parameters in order to account for what is known about ASM mass increase in health and disease at present (Figure 3), under the hypothesis that asthma is characterized by a temporary increase in the switching rate $c \to p$ during exacerbation events.

An obvious extension of the analysis above would be to study if and how the conclusions are modified if another rate parameter is assumed to undergo spike increases during asthma attacks. In a later stage, provided sufficient experimental data become available, it would be a very valuable achievement to be able to integrate our "ASM proliferation module" into a broader network of signalling pathways; in particular, to link the time variation of the rate parameters to the dynamics of inflammatory mediators and growth factors, since they are ultimately responsible for these variations (see, e.g., [20]). As proliferation occurs, there is also of course rearrangements of the muscle cells, and migration takes place, in particular toward the lumen [32]. These spatial aspects should

also be incorporated into the model at some stage, for instance by extending the ODE to a reaction-diffusion PDE. Note that it could also be very beneficial to consider discrete alternatives to these continuous modelling approaches, such as a cellular automaton description, as it is particularly appropriate for population evolution problems.

Clearly, more experimental data is also needed to go further. As was mentioned during the problem presentation, what is known about ASM mass increase in asthma is largely qualitative and what is unknown is largely quantitative. As proliferation is concerned, we were initially provided with a single number, the increase in ASM cell number *in vitro* over 48 hours upon growth factor stimulation (C. Billington, unpublished work), without knowing exactly when this rate applies (i.e., far from or close to confluency). Indeed, the corresponding study was not designed to estimate proliferation rates, but we were told that additional more complete data would be very easy to generate. We became subsequently aware of two references giving 3-4 time points [23, 8], but this is still very little longitudinal data, and concern growth *in vitro*. *In vivo*, it is of course very difficult to obtain good longitudinal data, as it requires performing repeated biopsies on patients over lifetime. The study of Bai *et al.* [3] provides data on ASM mass evolution, but not on proliferation rates. We are aware of one study providing the percentage of proliferating cells in patients at one moment of their life (i.e, when they have had asthma for 24 years), and it is about 30% for severe asthma, against 12% for moderate asthma, and 6% for healthy [18]. In the intermittent $c \to p$ switching model above, the number of proliferating cells is substantial only during exacerbation events (Fig. 14). In the absence of longitudinal data, it is unfortunately impossible to say whether this is realistic or not.

As apoptosis is concerned, we know from the problem presentation that ASM is fairly resistant to apoptosis *in vitro* [17, 15] , that some animals (rats) do show substantial ASM apoptosis *in vivo* (even in control specimen, which suggest a a rapid and dynamics turnover of tissues, since ASM mass is observed to be constant in control) [20], and that human show "minimal" ASM apoptosis *in vivo* (S. Johnson, unpublished work). However, for data on the percentage of cells that are "marked for apoptosis" to provide useful apoptosis rate informations, we would need to know what it means in terms of the time left for cells to live, and whether this data suffers from an important amount of variability or not.

As switching between the two populations is concerned, we do not know if data about phenotypic change rates exist, but it would already be helpful to know to what extent proliferating rates are (not) inherited *in vitro*. Also, it would be valuable to get a better understanding of how the proliferative and non-proliferative cell types relate to the synthetic and contractile phenotypes, as there is doubt that there is a one-to-one mapping between "contractile" and "non-proliferative" characters and between "synthetic" and "proliferative" characters (that is why we avoided referring to the "contractile" cell type in this work).

Finally, let us note that this study group work has focused on ASM mass increase in asthma due to cell hyperplasia, while cell hypertrophy could play a role in this mass increase as well, and could therefore also be the subject of future work.

4.2 ASM mass and lung function

The model for reduction of FEV_1 in Section 3.2 is intended only as a rough indication of how we can predict a reduction in airway radius. A more accurate prediction would be highly useful in the study of lung remodelling, as it would give us longitudinal in-vivo

information that we can link to ASM proliferation. Clearly to draw actual inferences we would need another model explaining how ASM proliferation relates to the reduction of airway calibre which may not be entirely straightforward.

The model we established makes a number of flawed assumptions; such that the branching of the human lungs is symmetric, that the pressure is constant over the second that the FEV_1 measurement is taken, that the airways can be treated as perfectly cylindrical, rigid tubes and that the only aspect of remodelling that contributes to decrease in asthmatic lung function is airway narrowing. Additionally we have only been able to model down to the tenth generation of the airways due to the limitations of the parameters found in literature. Finally the example we provided is highly simplified as it looks at airway narrowing only as a universally applied percentage reduction of airway radius and only looks at one starting initial 'lifetime peak' flow.

There are also a number of other possible factors at play here, for instance the increase of airway mucus in an asthmatic lung, the buckling of airways (and thereby further effective radius reduction) that may be experienced as a result of ASM proliferation, the increased likelihood of airway derecruitment as a result of this type of buckling and effects on lung tissue compliance/friction may all be reasonably expected to play a role in FEV_1 reduction.

This work could be greatly improved by a number of means. Firstly there already exists a fairly large range of literature in this field, including a number of established models, which will have application to this work. An in-depth literature review was beyond the scope of the study group, but would probably provide a number of insights into the problem. It would also likely be possible to create a model accounting for, or avoiding, many of the limitations we have described above. For instance there are cases in the literature of models that numerically solve the Navier Stokes equations over anatomically accurate 3D representations of lungs - whilst this is far beyond what is required, or indeed practical, for this work, it does show that very refined models of fluid flow through the lungs can be created. Overall, this is not a small project and there are many individual facets of this work that could yield meaningful results - the step that we are currently missing, that of linking or assimilating the data from these physiological predictions to models of cellular processes is the one that could potentially present the greatest prize - it would provide a simple and effective tool to obtain currently intractable, in-vivo information via non-invasive means.

4.3 Potential to reduce animal use

One of the objectives of setting this challenge was to explore if mathematical modelling could reduce animal use in understanding ASM remodelling in asthma. By integrating existing in vitro, animal and human data it has been possible to develop two models which could provide information not previously obtainable in animal models. More precisely, the described challenge utilised pre-existing in vitro data generated from human cells (rates of proliferation and apoptosis) in addition to previously reported human in vivo clinical data (longitudinal lung function studies) and human ex vivo datasets (previously published ASM mass measured via immunostaining of airway sections and preliminary data regarding the presence / absence of proliferative / apoptotic cells in airway sections) to develop 1) a cell-population model which accounts for ASM growth in health and disease, and 2) a model of airflow in the airway tree which is a first attempt at quantifying the effect of a reduction in airway calibre (due to remodelling) on lung function (FEV_1).

Comparing the generated modelling information with pre-existing data on the airway remodelling and altered lung function observed in animal models of chronic asthma and simulating experimental protocols may help experimentalists decide (A) what in vivo experiments it would be useful to do to address specific questions and to predict possible outcomes and (B) to predict whether or not an experiment will be able to answer the question under consideration.

As the integrated knowledge represented in the models continues to increase, the number of experiments, and therefore the number of animals used, will decrease. There is already proof of this happening in other areas of asthma research and drug discovery [27]. However, mathematical modelling approaches rely on the accuracy and extent of the existing knowledge base to populate them. A great deal more information exists in the literature to develop further the complexity of the current models described here, but it is clear gaps in knowledge still exist. In the short term more experimental data from in vitro and in vivo (human and animal) models will be required to validate these approaches and to obtain more information to increase their reliability and their ability to predict the in vivo situation.

5 Acknowledgements

We would like to thank first Dr Charlotte Billington, Prof Ian Hall, and Prof Simon Johnson for providing us with their invaluable experimental expertise during the study week. We also thank Prof Oliver Jensen, Prof Colin Please, Dr Markus Tindall, Kyriaki Giorgakoudi, Amy Smith and Katie Butler for their useful and stimulating contributions. We are of course also very grateful to the NC3Rs, and in particular to Dr Anthony Holmes, for submitting this problem to the 11th MMSG. Finally, we thank the MMSG organisers for facilitating and coordinating the week events.

References

[1] J. Lowe A. Stevens. *Human Histology third edition.* Elsevier Mosby, Philadelphia, 2005.

[2] AsthmaUK. For journalists: key facts & statistics, 2010.

[3] Tony R. Bai, Jamie Cooper, Tim Koelmeyer, Peter D. Pare, and Tracey D. Weir. The effect of age and duration of disease on airway structure in fatal asthma. *Am. J. Respir. Crit. Care Med.*, 162(2):663–669, 2000.

[4] Peter J. Barnes. New drugs for asthma. *Nat Rev Drug Discov*, 3:831–844, 2004.

[5] J. H. T. Bates. *Lung mechanics: an inverse modeling approach.* Cambridge University Press, 2009.

[6] Celine Bergeron, Wisam Al-Ramli, and Qutayba Hamid. Remodeling in asthma. *Proc Am Thorac Soc*, 6(3):301–305, 2009.

[7] B. S. Brook, S. E. Peel, I. P. Hall, A. Z. Politi, J. Sneyd, Y. Bai, M. J. Sanderson, and O. E. Jensen. A biomechanical model of agonist-initiated contraction in the asthmatic airway. *Respiratory Physiology & Neurobiology*, 170(1):44–58, 2010.

[8] Michelle L. D'Antoni, Chiara Torregiani, Pasquale Ferraro, Marie-Claire Michoud, Bruce Mazer, James G. Martin, and Mara S. Ludwig. Effects of decorin and biglycan on human airway smooth muscle cell proliferation and apoptosis. *American Journal of Physiology - Lung Cellular and Molecular Physiology*, 294(4):L764–L771, 2008.

[9] Graham M. Donovan and Merryn H. Tawhai. A simplified model of airway narrowing due to bronchial mucosal folding. *Respiratory Physiology & Neurobiology*, 171(2):144–150, 2010.

[10] M. Ebina, H. Yaegashi, R. Chiba, T. Takahashi, M. Motomiya, and M. Tanemura. Hyperreactive site in the airway tree of asthmatic patients revealed by thickening of bronchial muscles. a morphometric study. *Am Rev Respir Dis*, 141(5 Pt 1):1327–32, 1990.

[11] David Elad, Roger D. Kamm, and Ascher H. Shapiro. Choking phenomena in a lung-like model. *Journal of Biomechanical Engineering*, 109(1):1–9, 1987.

[12] Duncan F and Rogers. The airway goblet cell. *The International Journal of Biochemistry & Cell Biology*, 35(1):1 – 6, 2003.

[13] C.D. Richards G. Pocock. *Human Physiology-The Basis of Medicine third edition.* Oxford University Press, Oxford, 2006.

[14] Pierre-Olivier Girodet, Annaig Ozier, Imane Bara, Jose-Manuel Tunon de Lara, Roger Marthan, and Patrick Berger. Airway remodeling in asthma: New mechanisms and potential for pharmacological intervention. *Pharmacology & Therapeutics*, 130(3):325–337, 2011.

[15] Andrew J. Halayko and Julian Solway. Invited review: Molecular mechanisms of phenotypic plasticity in smooth muscle cells. *Journal of Applied Physiology*, 90(1):358–368, 2001.

[16] Rabih Halwani, Jehan Al-Abri, Marianne Beland, Hamdan Al-Jahdali, Andrew J. Halayko, Tak H. Lee, Saleh Al-Muhsen, and Qutayba Hamid. Cc and cxc chemokines induce airway smooth muscle proliferation and survival. *The Journal of Immunology*, 186(7):4156–4163, 2011.

[17] Kimm J. Hamann, Joaquim E. Vieira, Andrew J. Halayko, Delbert Dorscheid, Steven R. White, Sean M. Forsythe, Blanca Camoretti-Mercado, Klaus F. Rabe, and Julian Solway. Fas cross-linking induces apoptosis in human airway smooth muscle cells. *American Journal of Physiology - Lung Cellular and Molecular Physiology*, 278(3):L618–L624, 2000.

[18] Muhannad Hassan, Taisuke Jo, Paul-André Risse, Barbara Tolloczko, Catherine Lemière, Ronald Olivenstein, Qutayba Hamid, and James G. Martin. Airway smooth muscle remodeling is a dynamic process in severe long-standing asthma. *Journal of Allergy and Clinical Immunology*, 125(5):1037–1045, 2010.

[19] Brian E. Heard and Suraiya Hossain. Hyperplasia of bronchial muscle in asthma. *The Journal of Pathology*, 110(4):319–331, 1973.

[20] Stuart J. Hirst, James G. Martin, John V. Bonacci, Vivien Chan, Elizabeth D. Fixman, Qutayba A. Hamid, Berenice Herszberg, Jean-Pierre Lavoie, Clare G. McVicker, Lyn M. Moir, Trang T. B. Nguyen, Qi Peng, David Ramos-Barbón, and Alastair G. Stewart. Proliferative aspects of airway smooth muscle. *Journal of Allergy and Clinical Immunology*, 114(2, Supplement):S2–S17, 2004.

[21] Anthony M. Holmes, Roberto Solari, and Stephen T. Holgate. Animal models of asthma: value, limitations and opportunities for alternative approaches. *Drug Discovery Today*, 16(15-16):659–670, 2011.

[22] A. L. James, T. R. Bai, T. Mauad, M. J. Abramson, M. Dolhnikoff, K. O. McKay, P. S. Maxwell, J. G. Elliot, and F. H. Green. Airway smooth muscle thickness in asthma is related to severity but not duration of asthma. *European Respiratory Journal*, 34(5):1040–1045, 2009.

[23] Peter R. A. Johnson, Michael Roth, Michael Tamm, Margaret Hughes, Qi Ge, Greg King, Janette K. Burgess, and Judith L. Black. Airway smooth muscle cell proliferation is increased in asthma. *Am. J. Respir. Crit. Care Med.*, 164(3):474–477, 2001.

[24] K.-H. Kuo, A.M. Herrera, and C.Y. Seow. Ultrastructure of airway smooth muscle. *Respiratory Physiology & Neurobiology*, 137(2-3):197 – 208, 2003.

[25] Peter Lange, Jan Parner, Jorgen Vestbo, Peter Schnohr, and Gorm Jensen. A 15-year follow-up study of ventilatory function in adults with asthma. *New England Journal of Medicine*, 339(17):1194–1200, 1998.

[26] T. Mauad, E.H. Bel, and P.J. Sterk. Asthma therapy and airway remodeling. *Journal of allergy and clinical immunology*, 120(5):997–1009, 2007.

[27] C. J. Musante, Annette K. Lewis, and Kevin Hall. Small- and large-scale biosimulation applied to drug discovery and development. *Drug Discovery Today*, 7(20):s192–s196, 2002.

[28] D C Savage. Microbial ecology of the gastrointestinal tract. *Annual Review of Microbiology*, 31(1):107–133, 1977.

[29] Malcolm R. Sears, Justina M. Greene, Andrew R. Willan, Elizabeth M. Wiecek, D. Robin Taylor, Erin M. Flannery, Jan O. Cowan, G. Peter Herbison, Phil A. Silva, and Richie Poulton. A longitudinal, population-based, cohort study of childhood asthma followed to adulthood. *New England Journal of Medicine*, 349(15):1414–1422, 2003.

[30] Gulshan Sharma and James Goodwin. Effect of aging on respiratory system physiology and immunology. *Clinical Interventions in Aging*, 1(3):253âĂŞ260, 2006.

[31] J. J. Shin, D. Elad, and R. D. Kamm. *Biological flows*, chapter Simulation of forced breathing maneuvers, pages 287–313. Springer, 1995.

[32] N. Takeda, Y. Sumi, D. PrÃľfontaine, J. Al Abri, N. Al Heialy, W. Al-Ramli, M. C. Michoud, J. G. Martin, and Q. Hamid. Epithelium-derived chemokines induce airway smooth muscle cell migration. *Clinical & Experimental Allergy*, 39(7):1018–1026, 2009.

[33] E. Weibel. *Morphometry of the human lung*. Springer-Verlag, Berlin, 1963.

[34] Barry R. Wiggs, Constantine A. Hrousis, Jeffrey M. Drazen, and Roger D. Kamm. On the mechanism of mucosal folding in normal and asthmatic airways. *Journal of Applied Physiology*, 83(6):1814–1821, 1997.